

Postsynthetic Surface Functionalization, Encapsulation, and Releasing Studies of a Novel Polymer Nanocapsule

Duangruthai Sridaeng,¹ Jacob J. Weingart,² Nuanphun Chantarasiri,¹ Jiang Zhe,³ J. Jack Hu²

¹Program in Petrochemistry, Supramolecular Chemistry Research Unit, Department of Chemistry, Faculty of Science, Chulalongkorn University, Bangkok 10330, Thailand

²Department of Chemistry, The University of Akron, Akron, Ohio 44325

³Department of Mechanical Engineering, The University of Akron, Akron, Ohio 44325

Received 29 June 2009; accepted 12 November 2009

DOI 10.1002/app.31755

Published online 23 March 2010 in Wiley InterScience (www.interscience.wiley.com).

ABSTRACT: Postsynthetic surface functionalizations of the amphiphilic poly(allyamine)-*g*-poly(*t*-butylacrylate) nanocapsule of 50–100 nm diameters are reported. The hydrophobic poly(*t*-butylacrylate) surface of the polymer nanocapsules were successfully functionalized with poly(acrylate) and poly(ethylene glycol). These new nanocapsules were investigated for their water dispersibility, encapsulation and controlled releasing properties with fluorescein, an anionic fluorescence probe, and 5-fluorouracil, an anticancer drug as the model compounds.

The postsynthetic surface functionalization approach of the cross-linked polymer nanocapsules shows promise for improving the biocompatibility and aqueous dispersibility of the nanocapsules without disrupting the encapsulation and releasing properties of the polymer nanocapsules. © 2010 Wiley Periodicals, Inc. *J Appl Polym Sci* 117: 706–713, 2010

Key words: multifunctional nanoparticle; polymer nanocapsule; controlled release; drug delivery

INTRODUCTION

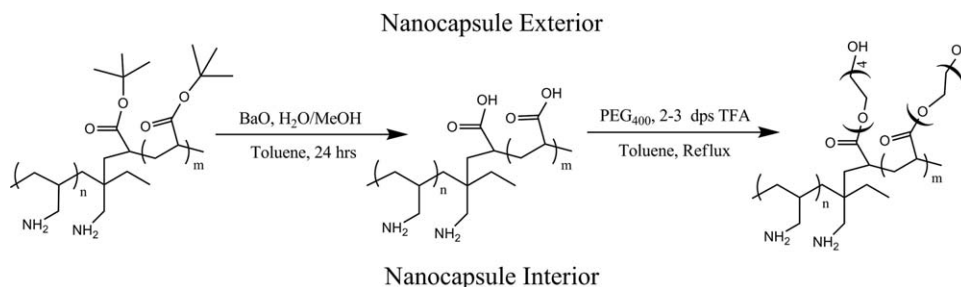
Nanotechnology focusing on the understanding and application of supramacromolecular structures has lead to implementation of various materials within the field of medicine. One emerging area of interest is the use of nanoparticles for targeted therapeutic delivery due to the favorable size and surface functionalities of various synthetic nanomaterials.¹ Whether the reagent is one used for imaging, chemotherapy, or both, the use of nanoparticles for targeted reagent delivery offers a series of advantages over the traditional small molecular medicines. These carriers are advantageous in the fact that they are similar in size to lipoproteins, and a number of other naturally occurring transport systems, as well as biocompatible through synthetic manipulation of the outer shell, aiding in the stability of otherwise sensitive or insoluble reagents.² In addition, the potential of incorporating targeting ligands on the outer surfaces of the nanocapsules can not only offer directed delivery reducing

overall body distribution, but can also provide sustained release within the targeted tissues specific to the actions of the chemotherapeutic reagents.^{1,2} This maximizes the dose of the reagent at the target site while minimizing side effects that are often caused by a broad biodistribution as seen in individuals treated by means of conventional chemotherapy.³ Typically, these nanocarriers are produced from smaller building blocks or even small molecular monomers by molecular recognition and self-assembling similar to the packaging of biological particles such as viral particles and small membrane vesicles. The use of synthetic building blocks is preferred to reduce the potential of rapid bioabsorption and immunosensitization of the nanoparticles. For example, the use of amphiphilic block copolymers as the building blocks has received much attention.⁴ Well-defined nanosized micelles can form spontaneously in water from polymers with well-controlled segments and molecular architectures. Nanocapsules arise from the subsequent covalent cross-linking of the building blocks followed by selective chemical degradations of the hydrophobic core segments.^{5–7} With such nanocapsules, the type of monomers as well as length of the crosslinkers used in the polymerization process allow for manipulation of properties in terms of biodegradability, swelling kinetics, and release rates. This also allows for the construction of nanocarriers that can incorporate both hydrophilic and hydrophobic drugs with adjustable release rates. In typical cases, diblock

Correspondence to: J. J. Hu (jhu@uakron.edu).

Contract grant sponsor: US National Science Foundation; contract grant numbers: DBI-0649798, ECCS-0708540.

Contract grant sponsors: Thailand Government Research Fund (Golden Jubilee Ph.D. fellowship), UASF (Summer faculty research grant).



Scheme 1 Chemical modifications of the poly(allylamine)-g-poly(*t*-butylacrylate) nanocapsules.

and triblock copolymers allow the most precise control of forming nanocapsule structures for these purposes. However, the synthesis of well-defined block copolymers, the self-assembling, cross-linking and chemical formations of such nanocapsules remain daunting tasks in terms of scaling-up for practical uses. One such copolymer that has been widely investigated as an alternative in a variety of nanocapsule formulations is the amphiphilic block copolymer poly(allylamine), PAA, and its derivatives. Considering its structure, the free amines of PAA allow for the ionic complexation of the copolymer onto oppositely charged macromolecules as well as the formation of a variety self assembled polymer architectures dependent upon the moieties attached to the chain.^{8,9} This method though proven to stabilize such charged biomacromolecules as lipids and DNA in nanocapsule-like structures, is quite demanding requiring the rigorous changing of environmental conditions, such as salt concentration, to induce such formations.^{10,11} However, PAA has still remained attractive due to the fact that upon the formation of such aggregates, one can choose to polymerize it covalently attaching the polymer chain to the enwrapped structure or crosslink the polymer to ensure structural stability of the nanocapsule architecture.¹²⁻¹⁴

In our research, we sought to develop alternative methods that combine the supramolecular architectures of block copolymers and the efficiency of controlled radical polymerizations for polymer nanocapsules. We reported a method for producing amphiphilic comb-polymer materials, favorable towards large scale synthesis using inverse microemulsion radical polymerization with a novel waterborne radical initiation system.¹⁵ In this method the self-assembled comb polymer architecture, formed during the inverse microemulsion radical polymerization of *t*-butyl acrylate grafted to the waterborne macromolecular radical initiator containing poly(allylamine), was cross-linked *in situ* at the water/oil interface of the inverse microemulsions to form the desired polymer nanocapsules.

For the intended uses in biological applications, it is necessary to test the surface chemistry of this new type of materials for further functionalization. In this report, we demonstrate the postsynthetic surface functionalization strategy with two types of surface modifications. At first, the surface layer of the nanoparticles were found to be readily hydrolyzed to polycarboxylates under acid or basic conditions, and second, the surface layer can also be easily PEGylated using acid catalyzed esterification reaction with excess of oligo(ethylene glycol). Both surface functionalized nanocapsules were investigated for their water dispersibility, encapsulation and controlled releasing properties with fluorescein, an anionic fluorescence probe, and 5-fluorouracil, an anticancer drug as the model compounds. Through two simple synthetic steps (Scheme 1) the material was functionalized with oligo(ethylene glycol). PEGylation was chosen because of its use in various biomedical applications and as a surface coat in many nanoencapsulate systems.¹⁶ Though PEG is not biodegradable, it is nontoxic, nonantigenic and soluble in water with molecule weights up to 4000 being easily excreted in humans.¹⁷ The hydrophilic nature of this material, when attached to a surface of a nanomaterial, inhibits protein adsorption increasing overall blood retention.¹⁸ The additional PEG layer coating of the nanoencapsulate system may create three distinct phases in which a variety of drugs or imaging agents maybe loaded into. The interior of the nanocapsule containing basic amine groups should be positively charged in neutral pH, capable of loading more anionic species such as DNA and RNA. The cross-linked polymer backbone shell and PEG layers are more hydrophobic, provides a sink for hydrophobic guest molecules. To test this idea, the nanocapsules were loaded with the anionic imaging reagent, fluorescein, and the anti-cancer drug, 5-fluorouracil. Herein we reported the surface modification chemistry, dispersion/swelling properties, loading and controlled releasing profiles of these new polymer nanocapsules.

EXPERIMENTAL

Materials

t-Butyl acrylate (*t*-BA, Aldrich, 98%) and ethylene diacrylate (ED, Acros, 70%) were washed with NaOH (MERCK, 97%) 5% aqueous solutions to remove the radical polymerization inhibitors, and dried over anhydrous MgSO₄ (Fischer, 99%) overnight and stored at 12°C prior to uses. Poly(allylamine) (PAA, 20 wt % solution in water, *M_w* 17,000, Aldrich), H₂O₂ (30 wt % solution in H₂O, Aldrich), toluene (Fischer, 99.9%), buffer solution pH 7.40 (PBS, Fischer), poly(ethylene glycol) (PEG, *M_w* 400, Acros), trifluoroacetic acid (TFA, Acros, 99%), 5-fluorouracil (5-FU, Acros, 99%), fluorescein (Acros, 99%), and sorbitan monooleate (Span 80, Aldrich) were used as received.

Synthesis of the polymer nanocapsules

The synthesis of the polymer nanocapsules was achieved using the previously reported procedure.^{15,19} Briefly, a three-necked round-bottomed flask was equipped with a thermometer, a condenser, an argon inlet, and a magnetic stir bar. The flask was charged with PAA (0.2 g in 5 mL of water), *t*-BA monomer (4.5 mL), ED (0.7 mL in 5 mL toluene), H₂O₂ (1.0 mL), and Span 80 (0.17 g). The resulting mixture was sonicated (Fisher FS6) at room temperature for 30 min, resulting in an inverse emulsion that was at least stable for 20 min when sitting at room temperature. The round-bottomed flask was placed in an oil bath and was heated at 65°C ± 2°C for 4 h under constant argon purge and uniform stirring. After the reaction, 50% v/v of an ethanol/water solution (30 mL) was added to the reaction mixture to precipitate the polymer. A white/pale yellowish sticky solid was obtained after removing the solvents and drying under vacuum at room temperature (0.7 g). The sample displayed identical NMR and IR spectra as the previous reported samples. ¹H-NMR: 0.89 (d, 2H, (CH₂)_{*n*}), 1.26 (d, 2H, (CH₂)_{*n*}), 1.5 (m, 9H, C(CH₃)₃), 1.57 (m, 2H, (CH₂)_{*n*}), 2.04 (t, 2H, CHCH₂NH₂), 2.18 (d, 2H, CH₂NH₂). FTIR (cm⁻¹): 2928, 1727, 1636, 1407, 1296, 1272, 1176, 1077, 985, 809.

Hydrolyzation of the *t*-butyl ester of the polymer nanocapsule

The use of *t*-butyl ester as the acrylic monomer for the polymer nanocapsule synthesis was intended for two purposes. At first, the *t*-butyl group is hydrophobic, which facilitates the formation of the reverse microemulsions during the radical polymerization. Second, the *t*-butyl group is also well-known to be readily removed under basic or acidic conditions.²⁰

For example, hydrolysis of the *t*-butyl group was achieved by employing the following base catalyzed reaction: To a suspension of the polymer (100 mg) in toluene (10 mL) in a 50 mL round bottom flask equipped with a magnetic stirrer was added a solution of BaO (41 mg) in a mixed solvent of H₂O/MeOH (1.0 mL, 1 : 4). The reaction mixture was stirred at ambient conditions overnight. Afterwards, the reaction mixture was washed with HCl (1M) to precipitate the polymer. The resulting suspension was filtered and the polymer was collected. The solid polymer was washed with MeOH and then dried under vacuum. ¹H-NMR: 0.89 (d, 2H, (CH₂)_{*n*}), 1.26 (d, 2H, (CH₂)_{*n*}), 1.64 (m, 2H, (CH₂)_{*n*}), 2.04 (t, 2H, CHCH₂NH₂), 2.9 (d, 2H, CH₂NH₂), 3.0 (d, 2H, CH₂COO). FTIR (cm⁻¹): 2900, 1725, 1550, 1452, 1407, 1364, 1250, 1148.

Surface modification of polymer nanocapsules with poly(ethylene glycol)

Into a two-necked 50-mL round bottom flask equipped with a reflux condenser and a magnetic stirrer, was charged with the hydrolyzed polymer nanoparticle (36 mg), PEG (MW 400, 77 mg), TFA (1 drop), and toluene (anhydrous, 20 mL). The reaction mixture was refluxed under argon for 6 h. After refluxing the polymer was filtered, revealing a sticky yellowish solid mass of particles that were washed with MeOH and then vacuum freeze dried. This procedure was replicated for the addition of propargylic poly(ethylene glycol) to the polymer surface as well. ¹H-NMR: 0.88 (d, 2H, (CH₂)_{*n*}), 1.25 (d, 2H, (CH₂)_{*n*}), 2.4 (d, 2H, CH₂NH₂), 3.66 (t, 4H, (OCH₂CH₂O)_{*n*}), 3.77 (t, 2H, COOCH₂). FTIR (cm⁻¹): 2874, 1788, 1455, 1345, 1220, 1162, 951, 856.

Encapsulation of fluorescein into the polymer nanocapsules and release studies

The fluorescein-loaded nanoparticles were produced using dialysis methods.^{21,22} A total of 5.0 mg and 45 mg of the capsule polymer were dissolved in 50 mL of MeOH and then vortexed for 6 h at room temperature. Then the fluorescein-loaded nanoparticles were placed in a dialysis membrane (FisherBrand, cellulose) and soaked in water for 24 h. To determine the loading amount, 10 mg of the loaded nanoparticles were dispersed in 10 mL of phosphate buffer (1 mM, pH 7.4), and the mixture was shaken on a vortexer (Fisher) for 2 min. The formed emulsion was centrifuged and the aqueous phase was collected to determine the amount of fluorescein released via UV-vis spectroscopy over time.

Encapsulation of 5-fluorouracil into surface-modified polymer nanocapsules and release studies

Similarly to the previously used aforementioned methods, the polymer nanocapsules were dispersed in 2 mL and a predetermined amount of 5-fluorouracil, an anticancer therapeutic, was added to the solution. The nanoparticle-drug solution was stirred at room temperature for 6 h. The nanoparticles were then frozen by a freeze-dyer system to obtain the dried nanoparticles loaded with the drug. To determine the loading amount, 10 mg of 5-fluorouracil loaded nanoparticles were dispersed in 10 mL of phosphate buffer (1 mM, pH 7.4), and the mixture was shaken on a vortexer for 2 min. The formed emulsion was centrifuged and the aqueous phase was collected to determine the amount of 5-fluorouracil via UV-vis spectroscopy over time.

Spectroscopic and thermal analyzes

NMR analysis was performed using a Varian Gemini 300 NMR spectrometer. Characterizations of the polymer nanocapsules and resulting surface-modified nanoparticles were performed with CDCl_3 as the solvent and internal reference (7.27 ppm in $^1\text{H-NMR}$). FTIR analysis was performed with a Nicolet NEXUS 870 FT spectrometer. ATR sampling technique is exclusively applied with the Thunderdom Thermogravimetric analysis (TGA) was performed with a TGA Q500 (Q Advantage 2.8 TA) instrument. Differential scanning calorimetry (DSC) was performed with a DSA Q2000 (Q Advantage 2.8 TA) instrument. UV-vis spectra were recorded on an Oceanoptics USB4000 UV-vis spectrometer.

RESULTS AND DISCUSSION

For surface chemical modification studies, polymer nanocapsules were prepared by employing the previously reported method (Scheme 1).^{15,19} The chemical composition of the freshly made polymer nanocapsules was confirmed through $^1\text{H-NMR}$, FTIR analysis, and solvent dispersibility tests with respect to those published before.

Hydrolysis of the *t*-butyl group of the polymer nanocapsules was achieved by refluxing in a water/methanol mixture using $\text{Ba}(\text{OH})_2$, produced *in situ* from BaO , as the base catalyst.²⁰ As the reaction progressed, it can be observed that the initial more heterogeneous reaction mixture gradually turned into a more gel like mixture. The reaction mixture was then acidified and the polymer product was purified through dialysis and dried at ambient conditions. $^1\text{H-NMR}$ spectrum of the polymer product showed distinctive peaks at 0.8–1.3 ppm corresponding to

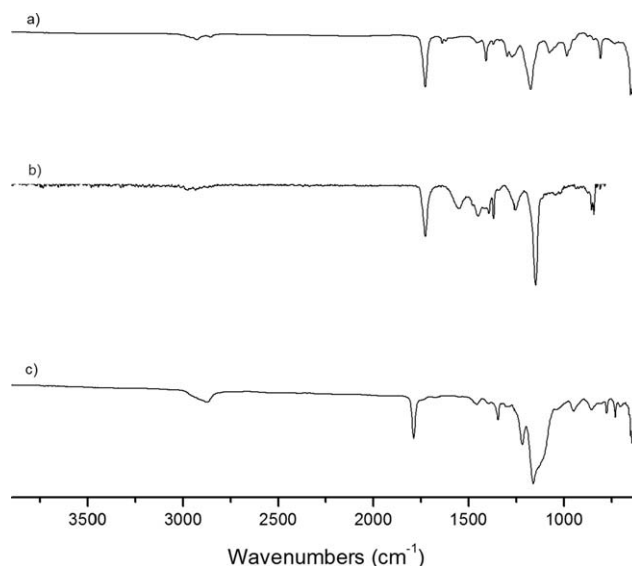


Figure 1 FTIR of the unmodified (a), hydrolyzed (b), and PEGylated (c) poly(allylamine)-g-poly(*t*-butylacrylate) polymer nanocapsules.

the hydrocarbon polymer backbone which remained. In contrast to the polymer nanocapsules before the hydrolysis, the peak at 1.5 ppm assigned to the *t*-butyl group disappeared in the product, indicating that it was successfully hydrolyzed. The peaks at 2.9 and 3.0 ppm were assigned to the methylenes next to a carbonyl and a tetra-coordinated amine ($-\text{NH}_4^+$).⁹ They appeared to be sharpened after the hydrolysis, supporting the notion that with the bulky *t*-butyl groups hydrolyzed these groups become more mobile and accessible to the solvents. This observation is also supported by the subsequent thermal analyzes. FTIR of the nanoparticles further confirmed the success of the synthetic modification with the disappearance of C—O—C stretching at 1176 cm^{-1} that is part of the ester, as well as a significant decrease in the intensity of the C—H stretching ranging from $2800\text{--}3000\text{ cm}^{-1}$, indicative of loss of the *t*-butyl group [Fig. 1(b)].

PEGylation of the polymer nanocapsules was achieved by attaching PEG_{400} to the polymer via an acid catalyzed esterification reaction with an excess of $-\text{OH}$ terminated PEG_{400} . The freeze dried product showed a distinctive $^1\text{H-NMR}$ signature at 3.6 ppm, which corresponds to the protons of the $-\text{OCH}_2\text{CH}_2\text{O}-$ segment of the PEG. This is further supported by FTIR analysis with an increase in intensity of the C—H stretching at 2874 cm^{-1} as well as the appearance C—O—C stretching at 1220 and 1162 cm^{-1} corresponding to the ester and ether moieties on the surface of the nanoparticles [Fig. 1(c)].

The two types of surface-modified polymer nanocapsules were subjected to thermometric analyzes. DSC thermograms were taken over the range of -25 to 120°C at a scan rate of $10^\circ\text{C}/\text{min}$. The data

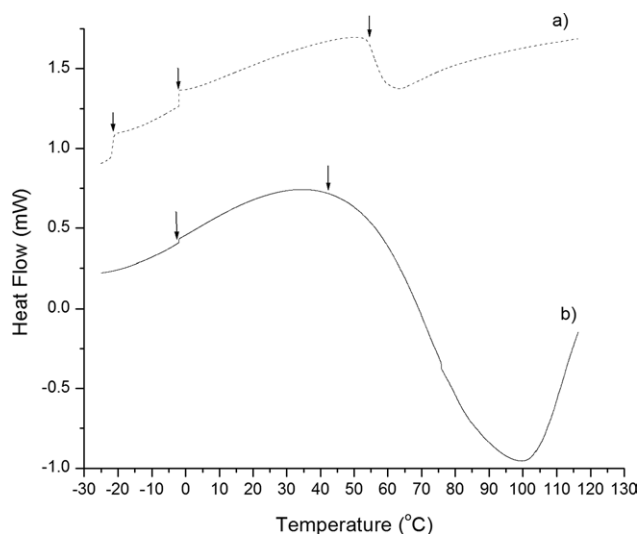


Figure 2 DSC measurements of hydrolyzed (a) and PEGylated (b) poly(allylamine)-*g*-poly(*t*-butylacrylate) polymer nanocapsules. Arrows indicating glass transition states (T_g s).

collected for the two types of material is shown in Figure 2. The DSC data of the original material exhibits two glass transitions (T_g s) representative of two polymer domains. The first T_g occurs at $\sim -1^\circ\text{C}$ was assigned to the poly(allylamine), PAA, segment which is in accordance with other published data, while the second T_g at $\sim 55^\circ\text{C}$ was assigned to the poly(*t*-butyl acrylate) segment.^{19,21} For the hydrolyzed material, both of these T_g s are well represented even with the conversion of the poly(*t*-butyl acrylate) segment to a poly(carboxylate) segment [Fig. 2(a)]. However, there appears to be a third T_g at $\sim -22^\circ\text{C}$. This maybe attributed to the fact that without the presence of the bulky *t*-butyl groups, the segments containing carboxylate groups are free to rotate along the polymer backbone. For PEG₄₀₀-coated coreshell material the T_g at $\sim -1^\circ\text{C}$ corresponding to the PAA segment remains the same. However, the T_g representative of the poly(*t*-butyl acrylate) segment is shifted to a lower temperature with the exchange of PEG for the *t*-butyl group of the ester. This shift of the T_g to $\sim 40^\circ\text{C}$ can be attributed to the amorphous nature of the PEG on the surface of the molecule [Fig. 2(b)].

TGA of the surface-modified polymer nanocapsules was also performed at a scan rate of $10^\circ\text{C}/\text{min}$ from 25 – 500°C . Similarly to unmodified polymer nanocapsules, the hydrolyzed material two distinct decomposition stages [Fig. 3(a)]. The first stage occurring at $\sim 250^\circ\text{C}$ is due to the loss of the carboxylate groups on the surface of the material representing 40% of the total weight of the material. The second stage occurring at $\sim 420^\circ\text{C}$ results in the decomposition of the internal segments of PAA, which represents 60%, the bulk, of the total weight

composition of the material. For the PEG₄₀₀-coated polymer nanocapsules material, as expected, there were three distinct decomposition stages [Fig. 3(b)]. The first decomposition stage begins at $\sim 160^\circ\text{C}$ and corresponds to the PEG₄₀₀ layer, which represents 25% of the weight of the material. The second stage at $\sim 250^\circ\text{C}$ is the decomposition of the carboxyl group of the ester to which the PEG₄₀₀ is attached. This portion of the material represents 25% of its weight. The remaining 50% of material left, the PAA segments, undergoes decomposition at $\sim 420^\circ\text{C}$.

Changes to the surface structure of the polymer nanocapsules lead to changes in behavior across a series of different solvents (Table I). Samples of the polymeric nanoparticles were exposed to solvent for 8 h at a time. It has been previously illustrated that the unmodified nanoparticles, due to the hydrophobic exterior attributed to the *t*-butyl groups of the ester, exhibited swelling in hydrophobic nonpolar solvents, such as toluene, over time.¹⁹ Upon hydrolysis of the *t*-butyl groups the surface of the polymer nanocapsules becomes more hydrophilic with formation of carboxylate anions. No longer exhibiting swelling in toluene, the material exhibits partial swelling in more polar organic solvents such as ethyl acetate, DMF and THF indicating some solubility. Yet, it still remained insoluble in water exhibiting little to no swelling. With the addition of a layer of PEG₄₀₀ to the surface of the polymer nanocapsules, the behavior of the nanocapsules significantly changes across the whole range of solvents tested with the exception of petroleum ether. This is due to the amphiphilic nature of the PEG₄₀₀ in the creation of a multilayered/multiphase nanoparticle as depicted in Scheme 1.

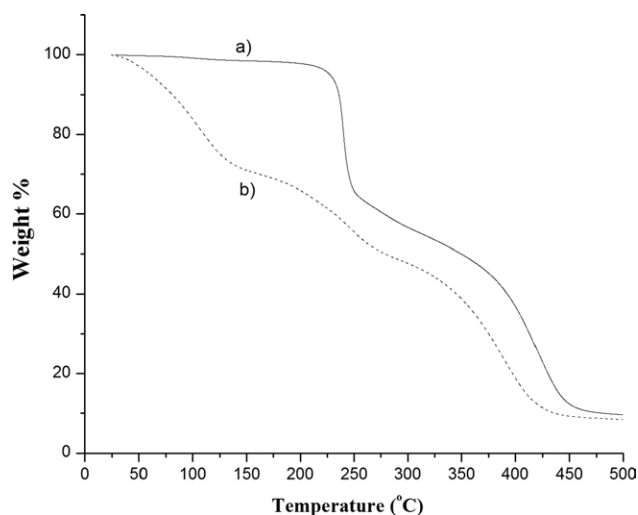


Figure 3 TGA measurements of hydrolyzed (a) and PEGylated (b) poly(allylamine)-*g*-poly(*t*-butylacrylate) polymer nanocapsules.

TABLE I
Behavior of the Polymer Nanocapsules Exposed to Different Solvents
Over an 8 h Period at 25°C

Solvents	Coreshell	Hydrolyzed coreshell	Hydrolyzed coreshell +PEG ₄₀₀
DMF	Insoluble	Swells	Swells
DMSO	Swells	Swells	Swells
Toluene	Swells	Insoluble	Swells
Dichloromethane	Swells	Insoluble	Slight swelling
Ethanol	Insoluble	Insoluble	Slight swelling
Ethyl acetate	Insoluble	Swells	Slight swelling
Water	Insoluble	Insoluble	Slight swelling
Petroleum ether	Insoluble	Insoluble	Insoluble
Acetone	Insoluble	Insoluble	Slight swelling
THF	Insoluble	Swells	Slight swelling
Diethyl ether	Insoluble	Insoluble	Slight swelling

The aforementioned spectroscopic and thermal characterizations provide support for the successes in the surface modifications of the polymer nanocapsules. The original PAA-*g*-poly(*t*-butyl acrylate) cross-linked comb copolymer core-shell architecture are shown to be robust and suitable for post synthetic surface modifications without losing the overall micelle morphology and dispensability. The results from two typical modifications demonstrate that the surface properties, including solubility and biocompatibility, of these nanocapsules can easily be manipulated to suit a number of uses. One use, as a controlled release nanocarrier for small molecule imaging and therapeutic agents, was further investigated.

When observing the release profiles of nanocapsules, one must consider the type of device category that it falls under. Typically, nanodelivery systems fall under two categories, matrix-based or membrane controlled devices. A matrix-based device is one in which the reagent is actually contained within the polymer matrix and is slowly released as the matrix degrades or activated by a change in the surrounding environment, such as pH. In membrane controlled devices, the drug resides in a reservoir adjacent to the polymer matrix backbone or shell which acts as the rate controlling membrane.²³ Our system, falling into the later category, should be a porous material due to its comb architecture. If this is so, then the release of the reagents from the core of these nanocapsules should be governed by diffusion following Fick's law. For this reason, the results of our work were fitted to the selected equation,²⁴

$$W_t/W_\infty = kt^n$$

where W_t/W_∞ is the fractional release at time t , k is the rate constant and exponent n , the diffusion coefficient. The diffusion coefficient is the factor that dictates the mechanism of diffusional transport

involved. When $n = 0.5$, this mechanism of transport is Fickian. When $n = 1$ or that in between, the release is considered zero order or anomalous.²⁵

Both types of surface-modified nanocapsules were loaded with small guest molecules, with known UV-vis absorbance spectra, by soaking the polymer nanocapsules in the solutions of the guest molecules in organic solvents. The polymer nanocapsules loaded with the guest molecules were then washed and dried for releasing studies. In the releasing studies, the loaded polymer nanocapsules were quantified and redispersed in aqueous buffer solutions with gentle shaking on a vortexer (Fisher). The amounts of the guest molecules diffused into the supernatant buffer solutions at each of the given time intervals were quantified via UV-vis absorbance measurements of the guest molecules in the supernatant liquids. The first reagent, fluorescein, was selected representative of an imaging reagent. For the hydrolyzed nanocapsules, releasing equilibrium was reached rapidly between the internal concentration of the reagent within the nanocapsules and the surrounding solution within ~ 1 min (Fig. 4). However, for the PEG₄₀₀-coated nanocapsules the amount of time required to attain equilibrium was nearly 3 times that of the hydrolyzed surface. Of the two modifications, it not only better fit the modeled equation with a more acceptable range of error but it behaves similarly to previously published results on such systems (Fig. 5).¹⁴ The discrepancy between the two different nanocapsules and their surfaces can be explained by the fact that for the hydrolyzed surface, there is a limited hydrophobic barrier through which the anionically charged fluorescein must travel through. This is not the case for the PEG₄₀₀-coated nanocapsules where the charged molecule must travel through the amphiphilic layer of poly(ethylene glycol).

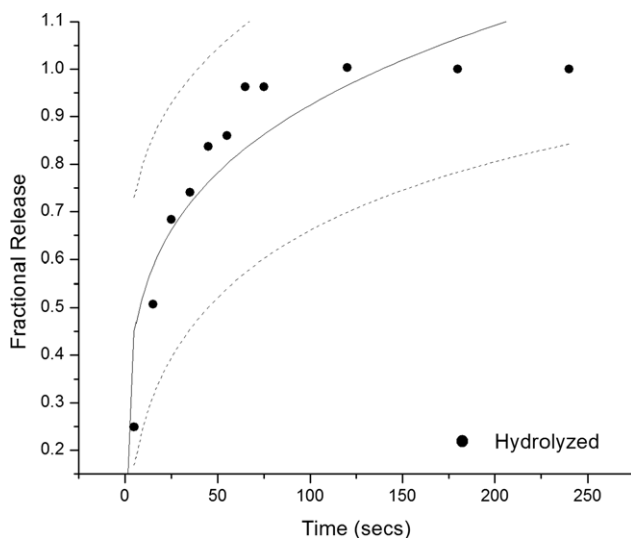


Figure 4 Fluorescein release profile for the hydrolyzed poly(allylamine)-*g*-poly(*t*-butylacrylate) polymer nanocapsules. Range of error denoted as space between dotted lines.

The second guest molecule tested was 5-fluorouracil, which represents a small molecule cancer reagent. Release until equilibrium from the hydrolyzed nanocapsules again occurred at a much faster rate than the PEG₄₀₀-coated nanocapsules and does not provide a proper fit to the modeled equation (Fig. 6). Though the amount of time for release until reaching equilibrium was significantly longer for the PEG₄₀₀-coated nanocapsules, the system does not appear to fit the modeled equation as well (Fig. 7). The release system itself appears biphasic having two different release rates and two distinct times.²⁶

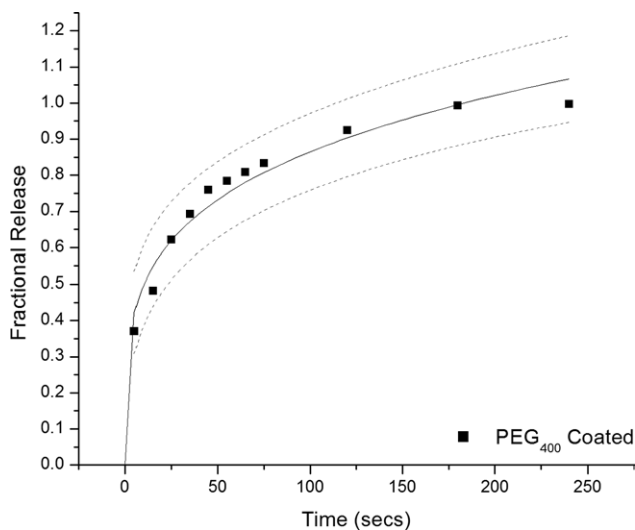


Figure 5 Fluorescein release profiles for the PEGylated poly(allylamine)-*g*-poly(*t*-butylacrylate) polymer nanocapsules. Range of error denoted as space between dotted lines.

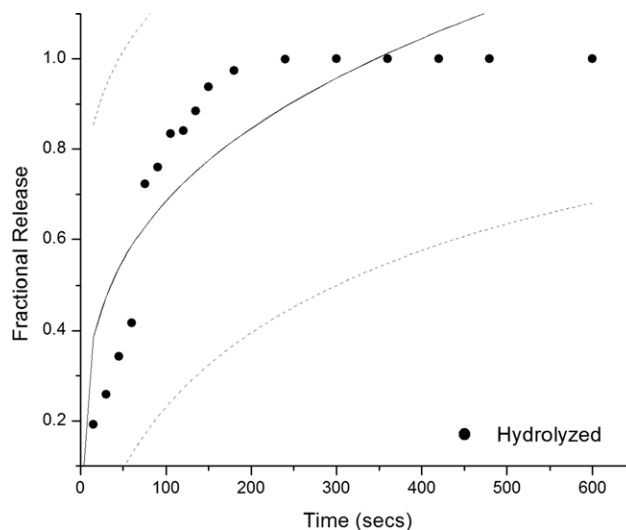


Figure 6 5-Fluorouracil release profiles for hydrolyzed poly(allylamine)-*g*-poly(*t*-butylacrylate) polymer nanocapsules. Range of error denoted as space between dotted lines.

This may stem from the fact that 5-fluorouracil has no moieties that exhibit a charge at physiological pH, 7.4. This being the case, the initial rate of release as the molecule diffuses through the hydrophobic backbone is dependent upon the initial swelling of the nanocapsule and should be greater than that of the second rate which is diffusion dependent as the molecule travels through the charged surface of the hydrolyzed nanocapsule or the amphiphilic surface of the PEG₄₀₀-coated nanocapsules.¹⁴ The results from fitting the data to the selected equation were obtained and are listed in Table II.

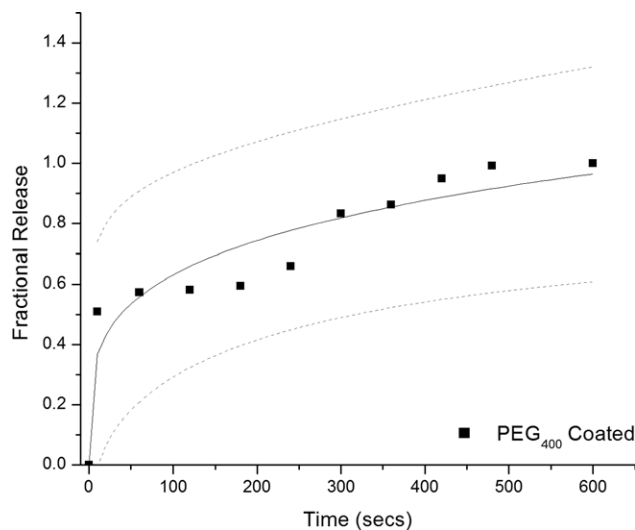


Figure 7 5-Fluorouracil release profiles for PEGylated poly(allylamine)-*g*-poly(*t*-butylacrylate) polymer nanocapsules. Range of error denoted as space between dotted lines.

TABLE II
The Releasing Results Fitted to $W_t/W_\infty = kt^n$

Nanocapsule type	Guest molecules	Parameters ^a		R^2
		k	n	
Hydrolyzed	Flourescein	0.3054	0.24047	0.81413
	5-Fluorouracil	0.16896	0.30416	0.74832
PEGylated	Flourescein	0.287	0.23952	0.95561
	5-Fluorouracil	0.21214	0.23674	0.79091

^a Obtained from non-linear fit using Microcal Origin version 6 software.

CONCLUSIONS

In conclusion, we found that the polymer nanocapsules are more effective carriers for negative charged small molecules in aqueous solutions at pH 7.4. This is most likely due to the quaternary ammonium groups that reside within the internal structure of the nanocapsule, which help to stabilize the negative charge. We attribute the fast releasing rates of the guest molecules mostly to the small size of the polymer nanocapsules (60–100 nm) used in this study. However, the results also indicated that the thin shells of the polymer nanocapsules may have defects that lowered the diffusion barrier of the guest molecules from releasing out of the capsule. We are in the process of increasing the molecular weight of the acrylic segment of the polymer nanocapsules to reinforce the shell structures. In addition, the aforementioned results are encouraging for us to proceed with the plan of using the polymer nanocapsules for negatively charged DNA and RNA deliveries.

References

- Panyam, J.; Labhasetwar, V. *Adv Drug Delivery Rev* 2003, 55, 329.
- Haag, R. *Angew Chem Int Ed* 2004, 43, 278.
- Babu, V. R.; Sairam, M.; Hosamani, K. M.; Aminabhavi, T. M. *Int J Pharm* 2006, 325, 55.
- Gillies, E. R.; Frechet, J. M. J. *Chem Commun* 2003, 1640.
- Wooley, K. L. *J Polym Sci Part A: Polym Chem* 2000, 38, 1397.
- Koh, A. Y. C.; Saunders, B. R. *Chem Commun* 2000, 2461.
- Li, Z. C.; Jin, W.; Li, F. M. *React Funct Polym* 1999, 42, 21.
- Murthy, V. S.; Rana, R. K.; Wong, M. S. *J Phys Chem B* 2006, 110, 25619.
- Thompson, C. J.; Ding, C.; Qu, X.; Yang, Z.; Uchegbu, I. F.; Tetley, L.; Cheng, W. P. *Colloid Polym Sci* 2008, 286, 1511.
- Werle, M.; Takeuchi, H. *Sci Pharm* 2008, 76, 751.
- Zhang, B.; Ji, W.; Liu, W.; Yao, K. *Int J Pharm* 2007, 331, 116.
- Lu, M. Z.; Lan, H. L.; Wang, F. F.; Wang, Y. J. *J Microencapsul* 2000, 17, 245.
- Chorny, M.; Fishbein, I.; Alferiev, I.; Levy, R. J. *Mol Pharm* 2009, 6, 1380.
- Crisante, F.; Francolini, I.; Bellusci, M.; Martinelli, A.; D'ilario, L.; Piozzi, A. *Eur J Pharm Sci* 2009, 36, 555.
- Sarkar, D.; El Khoury, J. M.; Lopina, S. T.; Hu, J. *Macromolecules* 2005, 38, 8603.
- Moghim, S. M.; Hunter, A. C.; Murray, J. C. *Pharm Rev* 2001, 53, 296.
- Rameez, S.; Alost, H.; Palmer, A. F. *Bioconjug Chem* 2008, 19, 1025.
- Yan, G. P.; Hua, L.; Cheng, S. X.; Bottle, S. E.; Wang, X. G.; Yew, Y. K.; Zhou, R. Z. *J Appl Polym Sci* 2004, 92, 3869.
- Sarkar, D.; El Khoury, J. M.; Lopina, S. T.; Hu, J. *J App Polym Sci* 2007, 104, 1905.
- Anderson, M. O.; Moser, J.; Sherrill, J.; Guy, R. K. *Synletters* 2004, 13, 2391.
- Zhang, Z.; Feng, S. S. *Biomacromolecules* 2006, 7, 1139.
- Huh, K. M.; Lee, S. C.; Cho, Y. W.; Lee, J.; Jeong, J. H.; Park, K. *J Controlled Release* 2005, 101, 59.
- Lee, A. J.; King, J. R.; Hibberd, S. *IMA J Math Appl Med Biol* 1998, 15, 136.
- Davidson, G. W. R.; Peppas, N. A. *J Controlled Release* 1986, 3, 265.
- Bajpai, A. J.; Choubooy, J. *J Appl Polym Sci* 2006, 101, 2323.
- Tzafiriri, A. R.; Lerner, E. I.; Flashner-Barak, M.; Hinchcliffe, M.; Ratner, E.; Parnas, H. *Clin Cancer Res* 2005, 826, 829.